Back to HAWAII – updating velocity low wavenumbers

Claudio Guerra, Carlos Cunha, Nelson Hargreaves and Julio Frigerio, Petrobras

Abstract

Recently, it was introduced a method to perform full waveform inversion (FWI) using the one-way wave equation (Guerra and Cunha, 2013), with 2D synthetic and field data examples. The method called HAWAII, acronym for **Ha**lf **Wa**veform **I**nversion, promises to be cheaper than the conventional FWI and uses the entire bandwidth present in data in contrast to the low-frequency range used in FWI. Comparing to the initially proposed, here we present a modification of the gradient, which allows us to introduce a low/medium wavenumber velocity correction. This consideration enables the method to be applied on highly imprecise initial velocity models.

Introduction

In the last years, research on velocity model definition has shifted from ray to wave methods, of which FWI (Tarantola, 1984) and WEMVA (Sava and Biondi, 2004) are the most popular ones.

FWI in 3D became a routine process, after a series of shortcuts were taken to overcome some serious limitations, like cycle skipping. Especially, the frequency/offset upscaling strategy that can lead to biased results, given that the earth model can be more sensitive to certain wavenumbers. To understand this issue, Figure 1 presents illumination maps at the base of salt computed for two different frequencies (7 Hz in Figure 1b and 70 Hz in Figure 1c) for a NAZ acquisition in the Santos Basin, Brazil. Top salt is showed in Figure 1a (blueish is shallower). Continuous line shapes highlight some of the high illumination features of the low frequency illumination, while the discontinuous ones do for the high frequency. Notice that there is strong correlation between high illumination for the low frequency and structural highs of the top salt. Moreover, there is weak correlation between illumination maps. The different illumination patterns implies that subsurface responds differently for different frequency ranges. In addition to this frequency dependency, it is hard to keep untouched low frequency signal during marine processing after swell noise removal, in spite of the efforts on the acquisition side to record reliable low frequencies. Therefore, it is desirable a method that does not strongly depends on the low frequency content.

To achieve this goal, we extend the cycle-skipping insensitive cross-correlation objective function of Luo and Schuster (1991), by using sliding windows in time. This data residual is back-projected to yield a migration-isochrone-like gradient (Macedo, 2014) with high wavenumber content.

Under a WEMVA perspective and inspired by the ideas of Almomin and Biondi (2012), we recognize that migration of data residuals of a FWI problem results in an image perturbation. An image perturbation, in turn, is the WEMVA data residuals. Computation of the WEMVA-velocity update yields a reflection-like gradient (Macedo, 2014) with low wavenumber content.

We end up with two gradient components, representing different scales of velocity-update wavenumbers. To make these different scales compatible will be explored in the future. Here, we focus on the WEMVA-derived component of the gradient.

Next, we review HAWAII as originally proposed and describe the computation of the new gradient component. Prior to that, we digress about the FWI gradient under the Born approximation. In the examples, we show the validity of our approach using simple synthetic 2D data.

Theory – FWI gradient

To support the methods described in the following sections, let us develop a different computation of the FWI gradient. Let us first consider Born modeling as the engine to generate the computed data. The corresponding FWI objective function can be written as

$$J_{FWI}(m) = \frac{1}{2}\|d - d_0\|^2 = \frac{1}{2}\|\mathbf{L}r - d_0\|^2, \quad (1)$$

where d_0 is the observed data, d is the modeled data, $\mathbf{L}$ is the linearized modeling operator, and r is an estimate of the reflectivity. Notice that $\mathbf{L}$ is linear with respect to the reflectivity, not to the model parameter. Reflectivity itself is a function of the model parameter, $r = r(m)$. Modeling is performed according to

$$d(\mathbf{x_s}, \mathbf{x_r}; \omega) = \omega^2 \int G_s(\mathbf{x_s}, \mathbf{x}; \omega) r(\mathbf{x}) G_r(\mathbf{x}, \mathbf{x_r}; \omega) d\mathbf{x}, \quad (2)$$

where ω is the radial frequency, $\mathbf{x_s}$, $\mathbf{x_r}$, and $\mathbf{x}$ are shot, receiver, and model position vectors, respectively. In the present case, G_s is the source one-way Green´s function and G_r is the receiver one-way Green´s function. The reflectivity r is obtained by deconvolving the wavelet as in Guerra and Cunha (2013).

The gradient of (1) with respect to the model parameter m is

$$\nabla J_{FWI} = \left(\frac{\partial \mathbf{L}}{\partial m} r + \mathbf{L}\frac{\partial r}{\partial m}\right)^* \Delta d, \quad (3)$$

where Δd is the data residual as defined in (1). Now, let us analyze the two terms between parentheses in (3).

Considering the modeling equation (2) and dropping the dependencies, we can rewrite (3) as

$$\nabla J_{FWI} = \left[\int \frac{\partial G_s}{\partial m} r G_r + G_s r \frac{\partial G_r}{\partial m} + G_s \frac{\partial r}{\partial m} G_r \mathbf{dx}\right]^* \Delta d. \quad (4)$$

The first two terms in the integrand relates to reflection responses due to secondary sources due to the presence of a model perturbation ($\partial/\partial m$), which defines the signal of these terms. The correlation of these events with the data residuals originates the isochrone-like part of the FWI gradient when the model perturbation is positioned on a reflector. The correlation of these events with the data residuals originates the rabbit-ear-like part of the gradient when the model perturbation is not positioned on a reflector. In the third term, brought to light due to the Born modeling consideration in (1), the partial derivative corresponds to the WEMVA-tomographic operator. The gradient of the original HAWAII corresponds to the first two terms with the model perturbation located on the reflector. In this paper, we propose to add the second term.

Method – Original HAWAII

HAWAII shares the same theoretical background of the wave-equation traveltime inversion of Luo and Schuster (1991). It is an optimization problem in which traveltime differences between the observed data (d_0) and the modeled data (d) are minimized. In our approach, data d are computed using Born modeling, according to (2).

Here, we aim at minimizing, in the l_2 sense, the traveltime differences between the observed and the modeled data. The traveltime differences are determined by measuring the lag $\Delta\tau$ of the maximum cross-correlation ϕ

$$\phi(\mathbf{x_s}, \mathbf{x_r}, \tau) = \int d_0(\mathbf{x_s}, \mathbf{x_r}, t+\tau) d(\mathbf{x_s}, \mathbf{x_r}, t) dt. \quad (5)$$

The mathematical representation of the problem does not change; irrespective we use the windowed trace/trace correlation.

The objective function $J(v)$ is

$$J(v) = \frac{1}{2} \|\Delta\tau(\mathbf{x_s}, \mathbf{x_r})\|^2. \quad (6)$$

For the velocity update, we need to compute the gradient of (6) with respect to the velocity, using

$$\nabla J(\mathbf{x}) = \frac{\partial \Delta\tau}{\partial v} \Delta\tau, \quad (7)$$

which, after some algebra, reads for one frequency

$$\nabla J(\mathbf{x};\omega) = \int\int G_s^*(\mathbf{x_s}, \mathbf{x}; \omega) G_r^*(\mathbf{x}, \mathbf{x_r}; \omega) \widehat{d_0}(\mathbf{x_s}, \mathbf{x_r}; \omega) d\mathbf{x_s} d\mathbf{x_r}, \quad (8)$$

where $\widehat{d_0}(\mathbf{x_s}, \mathbf{x_r}; \omega) = d_0(\mathbf{x_s}, \mathbf{x_r}, t) \Delta\tau(\mathbf{x_s}, \mathbf{x_r}, t)$ and the asterisk represents complex conjugate. The final gradient is obtained after summing over all the frequencies. Notice that the gradient corresponds to the migration of the observed data weighted by the lag of the maximum cross-correlation. If this lag is zero, observed data and modeled data perfectly match, so the gradient is zero and no velocity update is required. This gradient will be used as input to computed the WEMVA-like gradient.

As the gradient strongly resembles reflectivity since it is basically migration of the observed data after weighting by the lag of the cross-correlation, we transform the reflectivity-like information of the back-projected residuals into a pseudo-impedance-like one by deconvolving the remaining wavelet and integrating (Rosa, 2010). This operation is expected (not proved) to accelerate convergence. The reasoning is that velocity is more related to impedance than to band-limited reflectivity. Huang et al. (2011) uses a similar approach by integrating the data residuals. However, these authors were aiming at getting rid of the cycle-skipping problem instead of conditioning the gradient. Figure 2 presents slices through 3D volumes, showing the updated velocity after the first iteration for an example in the Santos Basin, Brazil.

Method – WEMVA-like HAWAII

In the original HAWAII, gradient is computed at the zero-subsurface offset as it is in the conventional FWI. As already mentioned, prior to the transformation to pseudo-impedance and smoothing, this gradient is a residual image.

We recognize that this residual image can be used as the data residual for a WEMVA-like problem. WEMVA is formulated to yield the long-wavelength velocity update, which allows correcting for big velocity errors. Notice that, the signal of the migrated data residuals determines the signal of the low wavenumber WEMVA gradient. For completeness, in the following, we summarize the WEMVA theory. More details can be obtained in Sava and Biondi (2004).

WEMVA is an inverse problem in which one searches for the velocity model v that minimizes the objective function

$$J(v) = \frac{1}{2} \|\Delta I\|^2, \quad (9)$$

where $\Delta I = \Delta I(\mathbf{x}, \mathbf{h})$ is the prestack-image perturbation. The subsurface offsets are represented by $\mathbf{h}$. We do not compute a prestack image, since the velocity error is represented by the polarity of the image perturbation.

There are several ways to compute the image perturbation. For instance, Shen and Symes (2008) uses the differential semblance optimization – DSO, while Sava and Biondi (2004) apply prestack residual migration to maximize focusing and flatness in the angle-domain. Here, we compute ΔI by migrating data residuals of the original HAWAII. In the following, in spite of having the $\mathbf{h}$ dimension, consider the result of the spatial crosscorrelation only for the zero lag. The gradient of (9) with respect to velocity is

$$\Delta J(v) = \left(\frac{\partial \Delta I}{\partial v}\right)^* \Delta I \quad (10)$$

To compute (10), let us first consider that the image reads for one frequency ω

$$I(\mathbf{x}, \mathbf{h}) = D^*(\mathbf{x} - \mathbf{h}) U(\mathbf{x} + \mathbf{h}), \quad (11)$$

where D is the source downgoing wavefield and U is the receiver upgoing wavefield. We implicitly assume

summation over all the shots and receivers. By applying the chain rule on (8), one obtains the perturbed image

$$\begin{aligned}\Delta I(\mathbf{x},\mathbf{h}) &= \Delta D^*(\mathbf{x}-\mathbf{h})U(\mathbf{x}+\mathbf{h}) \\ &+ D^*(\mathbf{x}-\mathbf{h})\Delta U(\mathbf{x}+\mathbf{h}),\end{aligned} \quad (12)$$

where the propagation of the perturbed wavefields ΔD and ΔU is governed by the wave equations

$$\begin{cases} \left(\frac{\partial}{\partial z} \pm i\sqrt{\omega^2 s_0^2(\mathbf{x}) - |\mathbf{k}|^2}\right)\Delta P(\mathbf{x}) = P_{sc}(\mathbf{x}) \\ \Delta P(\mathbf{x})|_{z=z_{min}} = 0 \end{cases}, \quad (13)$$

where P stands for the donwgoing or upgoing wavefields. In these cases, the signal of the square root is plus or minus, respectively. The scattered wavefields P_{sc} are computed as

$$P_{sc}(\mathbf{x}) = \pm \frac{i\omega\Delta z}{\sqrt{1-\frac{|\mathbf{k}|^2}{\omega^2 s_0^2(\mathbf{x})}}} P(\mathbf{x}), \quad (14)$$

which are the linearized solution with respect to the background slowness s_0 of the scattering operator. Signal of the square root follows the same rule as above and P represents the background wavefields. Therefore, for one frequency, the gradient computation follows the steps:

1) Compute source and receiver background wavefields D and U for all depth steps;

2) From the maximum to the minimum depth:

2a) Convolve the background wavefields D and U with the perturbed image ΔI, accumulating the result in the perturbed wavefields ΔU and ΔD, respectively

2b) Propagate the perturbed wavefields one depth level above

2b) Compute the scattered wavefields D_{sc} and U_{sc} using (14)

2c) Correlate D_{sc} with ΔD and accumulate the result on the correlation of U_{sc} with ΔU, originating ΔJ.

Taking the negative of ΔJ gives the update direction.

Therefore, in WEMVA-like HAWAII, the gradient is obtained as follows: a) migrate data residuals; b) input this result as an image perturbation to the adjoint of the WEMVA tomographic operator; and c) scale and edit the resulting slowness perturbation.

In the next section, examples illustrate the application of this theory.

Examples

We first apply the theory on synthetic data, which corresponds to the sedimentary portion of the Sigsbee dataset. Input data results from Born modeling, using the Sigsbee smooth migration velocity as the background velocity and a reflectivity computed from the Sigsbee stratigraphic velocity. The input data has 33 shots 180 m apart, in the split-spread configuration, maximum offset of 6800 m, and the maximum frequency is 30 Hz. For the inversion, initial velocity corresponds to the modeling velocity scaled down by a factor of 0.90, except for the water layer, which velocity is kept unaltered. Figure 3 shows the evolution of the objective function. Figure 4 presents the initial image, the image computed with the final velocity model, and the image computed with the correct model. Notice the high focusing of the diffractors, which validates the quality of the final velocity model. Figure 5 presents angle gathers computed with these three velocity models. The flatness of the reflectors also validates the quality of the final velocity model. Figure 6 shows the velocity models.

Conclusions

We present a method to update the low wavenumber component of the velocity model in HAWAII. This method is prone to be adapted for the conventional FWI. Results are promising, and currently we are implementing it in 3D to apply on real data of the Santos Basin.

Acknowledgments

We would like to thank Petrobras, for allowing publishing this article.

References

Almomin, A. and Biondi, B., 2012, Tomographic Full Waveform Inversion: Practical and Computationally Feasible Approach: SEG Technical Program Expanded Abstracts 2012: 1-5.

Guerra, C., and Cunha Filho, C.A., 2013, Full-waveform inversion using the one-way wave equation, Expanded Abstracts of the 14th International Congress of the Brazilian Geophysical Society.

Huang, G., Wang, H., and Ren, H., 2011, Two New Gradient Precondition Schemes for Full Waveform Inversion, International Geophysical Conference, Shenzhen, China.

Luo, Y., and G.Schuster, 1991a, Wave equation traveltime inversion: Geophysics, 56, 645–653.

Macedo, D., 2014, Scattering-based decomposition of sensitivity kernels of acoustic full waveform inversion, PhD thesis, Universidade de Campinas, Campinas, Sao Paulo.

Rosa, 2010, Análise do sinal sísmico: Sociedade Brasileira de Geofísica (SBGf), 668pp.

Sava, P. and B. Biondi, 2004, Wave-equation migration velocity analysis-I: Theory: Geophysical Prospecting, 52, 593–606.

Shen, P. and W. W. Symes, 2008, Automatic velocity analysis via shot profile migration: Geophysics, 73, VE49–VE59.

Tarantola, A., 1984, Inversion of seismic reflection data in the acoustic approximation: Geophysics, 49, no.8, 1259-1266.

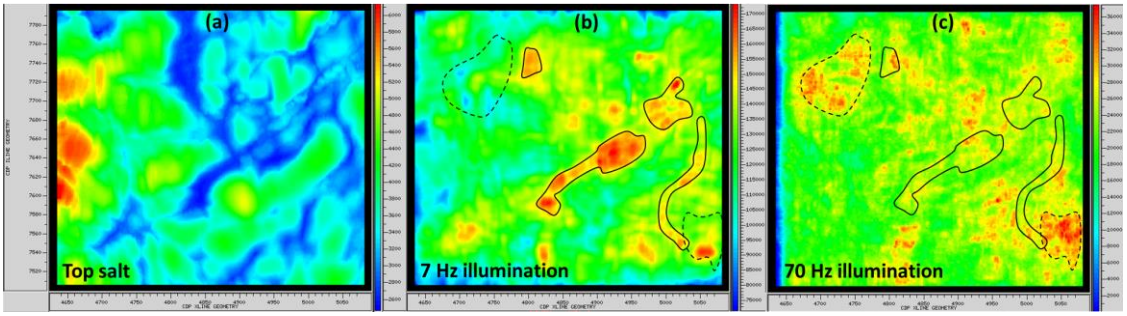

Figure 1 Frequency dependent illumination. Illumination computed for a NAZ acquisition for two distinct frequencies, illustrating the higher correlation of low frequency illumination (7 Hz) with structures of the top salt compared to the high frequency illumination (70 Hz). In this case, the salt layer acts as a wavenumber filter, making subsurface to respond differently for distinct frequencies.

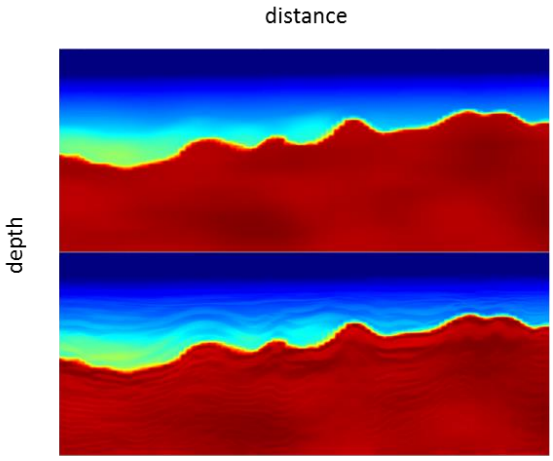

Figure 2 Comparison between the initial velocity (top) and the updated velocity (bottom) of the 1st iteration of the original HAWAII in the Santos Basin, Brazil.

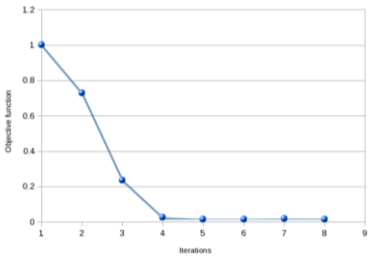

Figure 3 Evolution of the HAWAII objective function, using a WEMVA-like gradient, for the sediment portion of the Sigsbee model.

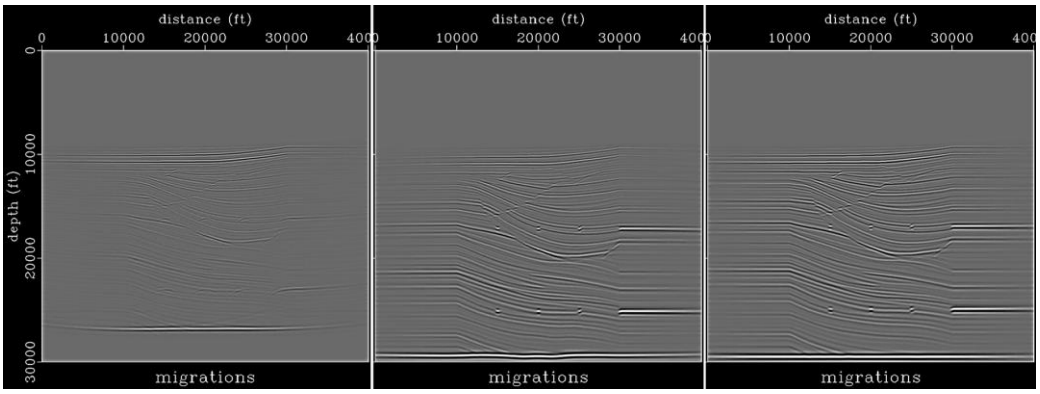

Figure 4 Frequency dependent illumination. Illumination computed for a NAZ acquisition for two distinct frequencies, illustrating the higher correlation of low frequency illumination (7 Hz) with structures of the top salt compared to the high frequency illumination (70 Hz). In this case, the salt layer acts as a wavenumber filter, making subsurface to respond differently for distinct frequencies.

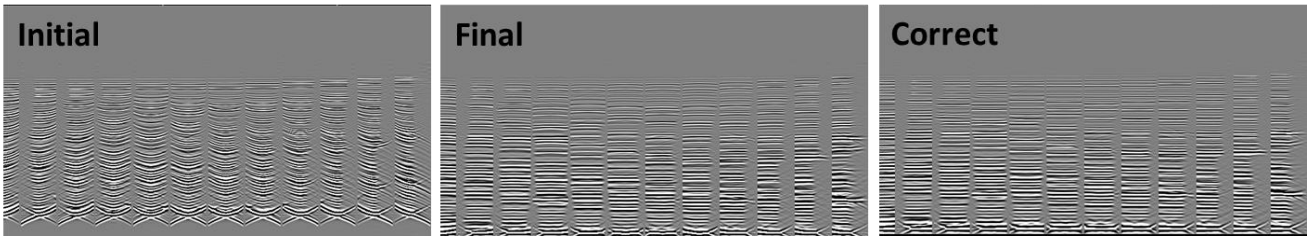

Figure 5 Angle gathers through the images computed with the initial (left), final (middle), and correct (right) velocity models.

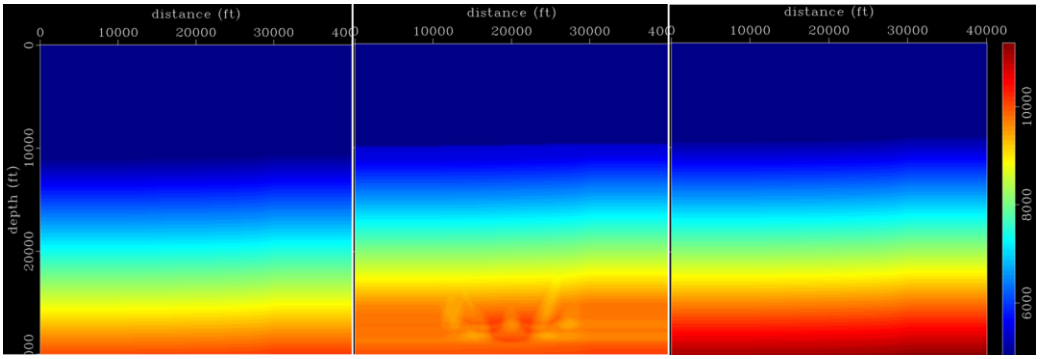

Figure 6 Initial (left), final (middle), and correct velocity models.